Ocean Sci. Discuss., https://doi.org/10.5194/os-2017-59
Manuscript under review for journal Ocean Sci.
Discussion started: 4 August 2017

Ocean Science
Discussions
Open Access

Transport Variability of the Brazil Current from Observations and a Model

Claudia Schmid [1] and Sudip Majumder [2]

[1]National Oceanic and Atmospheric Administration
[2]Cooperative Institute for Marine and Atmospheric Studies, University of Miami, Miami, FL, USA

Correspondence to: Claudia Schmid (claudia.schmid@noaa.gov)

Abstract.

Brazil Current transports from observations and a model are analyzed to improve our understanding of its structure and variability. The observed transports are derived from a three-dimensional field of the velocity in the South Atlantic covering the years 1993 to 2015 (hereinafter called Argo & SSH). The mean transport of the Brazil Current from 3.8±2.2 Sv (1 Sv is $10^6 m^3 s^{-1}$) at 25^{o}S to 13.9±2.6 Sv at 32^{o}S, which corresponds to a mean slope of 1.4±0.4 Sv per degree. The Hybrid Coordinate Model (HYCOM) has somewhat higher transports than Argo & SSH (5.2±2.7 Sv and 18.7±7.1 Sv at 25^{o}S and 32^{o}S), but these differences are small when compared with the standard deviations. Overall, the observed latitude dependence of the transport of the Brazil Current is in agreement with the wind-driven circulation in the super gyre of the subtropical South Atlantic. A mean annual cycle with highest (lowest) transports in austral summer (winter) is found to exist at selected latitudes (24^{o}S, 35^{o}S and 38^{o}S). The significance of this signal shrinks with increasing latitude, mainly due to the mesoscale and interannual variability. In addition, it is found that the interannual variability at 24^{o}S is correlated with the Southern Annular Mode and the Niño 3.4 index. A coupled EOF of the meridional transport and the sea level pressure is used to improve the understanding of the impact of these ocean indexes.

Copyright statement. TEXT

1 Introduction

The circulation in the South Atlantic has been studied extensively because it is an important part of the Atlantic Meridional Overturning Circulation, which consists of a northward transport of relatively warm and fresh upper ocean water of southern origin across the equator into the northern North Atlantic and a southward transport of relatively cold and salty deep water from the North Atlantic into the South Atlantic. A summary of the circulation in the South Atlantic as well as the pathways of the flow and its role in the Atlantic Meridional Overturning Circulation has been presented by Schmid (2014) and many others (references can be found in Schmid, 2014).

Herein, the focus is on the structure and variability of the Brazil Current, which is the western boundary current of the subtropical gyre in the South Atlantic and is largely governed by the Sverdrup Equation (Pond and Pickard, 1983). This gyre is part of the super gyre (Gordon et al., 1992; de Ruijter, 1982) which connects the subtropical circulation in the South Indian and South Atlantic Oceans. Mostly, the Brazil Current follows the shelf break quite closely, but it is impacted by mesoscale variability along its pathway that can give rise to meanders that separate it from the shelf break temporarily (e.g., Schmid et al., 1995; Biló et al., 2014; Mill et al., 2015; Lima et al., 2016). As the Brazil Current reaches the confluence with the Malvinas Current it is forced away from the shelf break and ultimately feeds into the eastward South Atlantic Current (e.g., Gordon, 1989; Garzoli, 1993; Maamaatuaiahutapu et al., 1998). Just prior to this eastward turn the southward transport increases due to the contribution from the Malvinas Current. Determining source and variability of the Malvinas Current (e.g., Vivier and Provost, 1999; Spadone and Provost, 2009) as well as what happens east of the confluence is beyond the scope of this study.

Another feature of the circulation in this region is a northward flow just east of the Brazil Current that originates near the confluence and is part of a recirculation cell that feeds back into the Brazil Current. This recirculation cell has been described earlier (e.g., Stramma, 1989) and has been called the Brazil Current Front (e.g., Peterson and Stramma, 1991) as well as the Brazil Return Current (e.g., Boebel et al., 1997).

The transports of the Brazil Current estimated in earlier studies vary from north to south (Fig. 1 shows them and provides the references). They are within 1 Sv to 7 Sv (1 Sv is $10^6 m^3 s^{-1}$) between 19^{o}S and 22.5^{o}S in the upper 400 to 500 m and increases to about 17 Sv at 28^{o}S as the vertical extent and strength of the Brazil Current increases. Farther south the Brazil Current transports are mostly in the range of 10 to 30 Sv. Most of the estimates from the earlier studies are based on quasi-synoptic sections, while some of them are based on time series from moorings with current meters or Inverted Echo Sounders (IES).

Previous studies of the temporal variability were typically limited in terms of the length of the time series (e.g., Rocha et al., 2013), the number of surveys (e.g., Mata et al., 2012) or derived as a time series at one location (e.g., Goni and Wainer, 2001), In addition, studies based on hydrographic measurements had to use a level of no motion or make assumptions about the barotropic flow (e.g. by prescribing a bottom velocity). The large variations in the transports from the previous studies as well as the limited knowledge about the temporal variability of the Brazil Current motivated this study on the characteristics and variability of this current at a wide range of latitudes.

Another motivation is that, as is well known, estimates of the Atlantic Meridional Overturning Circulation transports derived from various observational products and models often reveal similar amplitudes of the variability, but can have significant differences when the means are compared. For the north Atlantic, this was shown, for example, by Msadek et al. (2014). The same is the case in the South Atlantic. An important challenge for Atlantic Meridional Overturning Circulation transport calculations is the estimation of the transport in the western boundary current (the Brazil Current in the Subtropical South Atlantic). All estimates of this transport face the challenge of deriving the contributions on and often also near the shelf break. Typically, this challenge is resolved by using climatology (e.g., Garzoli et al., 2013; Majumder et al., 2016). The method used for estimating the transport of the Brazil Current is described in Appendix A and the uncertainty of the estimates based on Argo & SSH is quantified in Appendix B.

In summary, this study will build on the earlier results with the focus on improving the knowledge about the mean transport of the Brazil Current and its variability. In preparation for this analysis a monthly observations-based time series of three-dimensional fields of the horizontal velocity was derived. This time series covers 23 years with a horizontal grid resolution of 0.5°. The underlying dynamic of the observed variability on seasonal to interannual time scales is studied in conjunction with several ocean indexes and sea level pressure as a proxy for the wind field that is forcing the subtropical gyre.

The paper is organized as follows. Section 2 describes the data and methods. Sections 3 and 4 analyze the structure and variability of the Brazil Current transport. Section 5 summarizes the results.

Ocean Sci. Discuss., https://doi.org/10.5194/os-2017-59
Manuscript under review for journal Ocean Sci.
Discussion started: 4 August 2017

2 Data and methodology

Three oceanic data sets are used herein to derive an absolute three-dimensional geostrophic velocity field. They are profiles of temperature and salinity, subsurface velocities from float trajectories and sea surface heights. In addition, wind fields are needed to estimate the Ekman velocity that needs to be added to the geostrophic velocity prior to studying the circulation. Where these data sets come from and how they are used is described in the following.

The temperature and salinity profiles covering the years 2000 to 2015 come from an array of roughly 3000 floats that drift freely in the world ocean as part of the Argo project (the goal of 3000 active floats was reached in 2007). Details on the procedures regarding data acquisition and quality control were described in a previous study by Schmid (2014). The time period covered with hydrographic observations used in this earlier study has been extended by about 1.5 years. The number of profiles with temperature and salinity collected in the study region (Fig. 2) in the sixteen years (2000-2015) since the start of Argo that could be used herein is 81,627. Profile data are available throughout most of the study region (Fig. 2a) and this data coverage does not depend on the calendar month (not shown).

The trajectory data used for the estimation of the subsurface velocity are from Argo and WOCE floats that were active in January 26, 1989 to May 19, 2016. Details on the types of floats included in the data set can be found in Schmid (2014). As before, trajectories from floats drifting in the pressure range of 800 to 1100 dbar (930 of all floats) were used to derive the velocity field following the procedures described by Schmid (2014). As for the profiles, the coverage of the study region with high-quality velocities from the float trajectories is quite good (Fig. 2b) and the data coverage does not depend on the calendar month (not shown).

In addition daily sea surface height fields from AVISO are used (AVISO, France, 1996). The data set consists of delayed-time absolute dynamic topography on a $1/4^o$ grid covering the time period January 1993 to December 2015. The in situ data in conjunction with the sea surface height fields are used to derive absolute geostrophic velocities as described by Schmid (2014).

This product will be called Argo & SSH hereinafter. The volume transports of the Brazil Current is derived from these velocity fields as a monthly time series.

Wind fields from the NCEP reanalysis 2 (Kanamitsu et al., 2002) are used to derive the Ekman component of the transport, as in previous versions of the Argo & SSH data sets. Majumder et al. (2016) found that the Ekman transport computed from different wind products has only a small impact on the transports of the AMOC in the South Atlantic (their Figure 14).

Monthly velocity fields from the Hybrid Coordinate Ocean Model (HYCOM, (Chassignet et al., 2003) are obtained from Global 1/12^o Reanalysis and Analysis (GLBu0.08 experiments 19.0, 19.1, 90.9, 91.0, 91.1). This model has a Mercator-curvilinear grid with 32 levels and uses the Navy Coupled Ocean Data Assimilation (NCODA) system for assimilation. Although HYCOM is a Hybrid co-ordinate model where depth (‘z’) coordinates are used in the mixed layer and density in the lower layers, the output from the model is provided on depth coordinates.

Finally, the Southern Annular Mode (SAM, (Marshall, 2003) index, the Niño 3.4 index (Trenberth, 1997) and the Atlantic Multidecadal (AMO, e.g. (Enfield et al., 2001) and the sea level pressure from Modern Era Retrospective-analysis for Research and Applications (MERRA, Rienecker et al., 2011) are used for the analysis and discussion of the dynamics. The SAM index is defined as the normalized gradient of the zonal mean sea level pressure between 40^{o}S and 65^{o}S, the Niño 3.4 index is valid for the region 120^{o}W to 170^{o}W, 5^{o}S to 5^{o}N, and the AMO index is the detrended sea surface temperature anomaly in the Atlantic basin between the equator and 60^{o}N.

3 Mean characteristics of the Brazil Current transport

The mean transports from Argo & SSH for the upper 800 m, as derived from the monthly time series, reveals two bands of the westward southern South Equatorial Current which are part of the wind-driven subtropical gyre and feed into the Brazil Current at two main latitudes (near 22^{o}S and around 30^{o}S, Fig. 3a). Consistent with these westward transports, one can see a well developed Brazil Current along the western boundary south of about 28^{o}S, while this current is poorly developed in the mean transport field north of this latitude. A comparison with the mean surface velocity field presented by Oliveira et al. (2009) reveals a lot of similarity to the transport field derived herein: in the region south of about 26^{o}S Oliveira et al.'s Figure 4 shows a well developed Brazil Current while it is poorly defined in 23^{o}S to 25^{o}S where they find that the mean kinetic energy is lower than the eddy kinetic energy (Fig. 6 in (Oliveira et al., 2009) variability of the location as well as weakness of the Brazil Current in this area as already observed by Mata et al. (2012)

As is the case for Argo & SSH the HYCOM model also shows a strengthening of the Brazil Current in the region south of about 28^{o}S (Fig. 3b). Differences in the structure of the Brazil Current are visible when comparing HYCOM with Argo & SSH. Tendentially, the Brazil Current in the model is close to the 800 m isobath. North of 25^{o}S, the mean field from Argo & SSH has the southward flow about 2^o east of the 800 m isobath. HYCOM has a corresponding band of southward flow there, in addition to a more chaotic southward flow closer to the western boundary. This is consistent with the meandering of the Brazil Current in this region, for which section 2 presented evidence from earlier studies.

Details on the latitude dependence of the transport of the Brazil Current (which has been derived following the method described in Appendix A) are shown in Figure 4. For Argo & SSH and HYCOM the means are derived from monthly time series over the full time period. Before going into details it has to be noted that many earlier studies used varying layer thicknesses. North of 27^{o}S they are mostly smaller than 800 m and can be as small as 400 m. In support of this latitude dependence of the vertical extent of the Brazil Current the velocity structure in the Argo & SSH fields in this region indicates that the Brazil Current frequently is not well-defined below about 400 m. This is the reason for the statistics in Table 1 which show that the mean transport in 20^{o}S to 27^{o}S in the upper 400 m is almost as large as in the 0-800 m layer. Overall, the deeper layer (400-800 m) carries less than 19% of the transport in the upper 800 m in this latitude range (both for Argo & SSH and HYCOM). This is also in good agreement with the results of Rocha et al. (2014) as well as the dynamics governing wind-driven subtropical gyres (e.g., Luyten et al., 1983), their Figure 7). While the latter study is in the North Atlantic the method can be applied in the South Atlantic as has been done by Schmid et al. (2000), for example. Farther south the transport in the deeper layer contributes more than twice as much (32% for Argo & SSH, 36% for HYCOM in 39^{o}S to 33^{o}S, Table 1) to the transport in the upper 800 m. Based on these characteristics the transport in the upper 400 m will be used for the analysis in the region north of 27^{o}S from here on.

When comparing the mean meridional transport of the Brazil Current from Argo & SSH (black line in Fig. 4) with historical estimates (grey symbols in Fig. 4), one can detect a tendency for higher transports in some of the synoptic surveys. This is especially common north of 31^{o}S. Potential causes for such differences could be the inclusion or exclusion of the Ekman transport, differences of the vertical integration limits, representation of transports in the portion of the Brazil Current that is in shallow areas, and the impact of mesoscale variability. These will be discussed in the following.

The computation of the contribution of the Ekman transport to the transport of the Brazil Current reveals that the former is very small. Its magnitude amounts to less than 5% in 97% (99%) of the cases when compared with transports of the Brazil Current that exceed 1 Sv (2 Sv). Therefore, the Ekman contribution to the transport of the Brazil Current can be considered to be insignificant for these comparisons.

As stated above, the transports from earlier studies in the region north of 27^{o}S are estimated with varying layer thicknesses which mostly exceed 400 m. Because the transports from Argo & SSH are derived for the upper 400 m the transports from the earlier studies can be higher. However, this is unlikely to be the only reason for the differences (most of which are in the range if 2 to 6 Sv) because the 400-800 m layer contributes less than 19% to the transport in the upper 800 m (see above and Table 1).

An analysis of the contribution of the transport in shallow water to the total transport of the Brazil Current reveals that this contribution is small when compared with the differences between the independent transport estimates in Figure 4 (see Appendix B). The derived estimates indicate that this contribution does not exceed 2 Sv throughout the study region. Adding up the impacts of the shallow contribution and the layer thickness for the region north of 27^{o}S results in a combined effect that remains close to 2 Sv, which is still smaller than many of the differences between the transports from quasi-synoptic surveys and Argo & SSH that exist in this region.

Individual quasi-synoptic transects indicate that there is significant mesoscale variability in this latitude range (alternating 1-2 degree wide bands of southward and northward velocity with 20 to 30 cms^{-1} in XBT transects), both near 22^{o}S (Mata et al., 2012) and 25^{o}S (Garzoli et al., 2013, transects, not shown in detail) These meridional velocities are often twice as high as the monthly mean velocity in Argo & SSH. Therefore, one can get a roughly twice as large Brazil Current transport from individual transects for a given month and year when compared with the corresponding transport from a monthly mean velocity field. Taking an average of such quasi-synoptic transports can therefore result in a larger Brazil Current transport when compared with those from Argo & SSH. An example of the impact of that variability can be seen at 24.5^{o}S in Fig. 4 (gray dot with large error bar). Adding this effect to the other two (layer thickness and shallow water contributions) can explain most of the differences between the estimates from previous studies and Argo & SSH.

Transport estimates from individual hydrographic sections taken south of 27^{o}S mostly agree well with the means from Argo & SSH. However, a few exceptions exist, including the 51.4 Sv at 36^{o}S by Zemba (1991), which is about twice as high as the mean from Argo & SSH. This large discrepancy is not very worrisome, because the mesoscale activity at this latitude is very high due to the confluence of the Brazil Current and the Malvinas Current (which typically is found within about 3^o of 38^{o}S). Therefore, snapshots from quasi-synoptic sections can result in significantly larger transports than monthly averages.

More straightforward is a comparison of the mean transport estimates from the XBT lines (Garzoli et al., 2013, , gray dots in Fig. 4) with those from Argo & SSH, because multiple estimates from transects at a given latitude will reduce the impact of high variability. For example, at 35^{o}S the mean Brazil Current transport is 12.6±2.6 Sv from Argo & SSH. When keeping the variability at this latitude and the difference in observation period and method in mind, this result agrees very well with the 16.3±7.3 Sv derived from the XBT lines compiled by Garzoli et al. (2013) as well as the 14±7 Sv derived by Goni and Wainer (2001) based on a TOPEX/POSIEDON ground track crossing the Brazil Current near 35^{o}S (their Figure 7).

For the historical transport estimates the latitude dependence between 19^{o}S and 32^{o}S corresponds to a mean slope of about 1.6 Sv per degree (Fig. 1). However the characteristics in Figure 4 indicate that one can analyze the regions north and south of 25^{o}S separately. In the northern region (20^{o}S to 25^{o}S), the latitude dependence is relatively weak because the transports are not impacted by the strong westward flow reaching the boundary in the southern region (between 25^{o}S and 32^{o}S). The mean transport in the northern region from the historical studies is larger than the corresponding transport from Argo & SSH and also has a larger standard deviation (6.0±3.5 Sv versus 1.9±0.8 Sv). For Argo & SSH the largest time-averaged transport in this latitude range is 3.8±2.2 Sv at 25^{o}S. In addition, the mean of 1.9±1.1 Sv at 22^{o}S from Argo & SSH is in good agreement with the mean (2.3 Sv) derived near 22^{o}S by Mata et al. (2012). Overall, the difference between the independent estimates in the northern region is not very large when keeping the standard deviations in mind.

In the southern region the transport of the Brazil Current increases significantly from 3.8±2.2 Sv at 25^{o}S to 13.9±2.6 Sv at 32^{o}S for Argo & SSH, and from about 9 Sv to about 21 Sv for the historical estimates. For Argo & SSH and HYCOM slopes of the transport within this latitude range are estimated by applying a linear fit for each month of the full time series. These two sets of slopes are then used to derive their means and standard deviations. Due to the limited number of historical observations a different approach is used to derive the uncertainty of the slope. Four different estimates are derived by withholding some transport estimates from the calculation: slopes from a linear fit are calculated with and without considering transports lower than 4 Sv (such transports were measured near 25^{o}S, see Fig. 1) as well as with and without transports within 0.5^o north of

25^{o}S. The resulting slopes for the historical data range from 1.4 to 2.1 Sv per degree, with an average of 1.7±0.3 Sv per degree. For Argo & SSH and HYCOM the slopes are 1.4±0.4 Sv per degree and 1.9±0.9 Sv per degree, respectively. When taking the standard deviations into account, it can be concluded that the three estimates of the slope are in good agreement. This latitude-dependence is mainly due to the westward flow in the wind-driven subtropical gyre that reaches the boundary in this latitude range (Fig. 3).

In 33^{o}S to 39^{o}S the time-averaged transport from Argo & SSH fluctuates quite strongly around a mean of 17.3±3.5 Sv (Table 1, black line in Fig. 4). It is not likely that this is caused by changes in the southern South Equatorial Current, because most of the water transported by this current reaches the western boundary north of 33^{o}S (Fig. 3). One possible cause is the Brazil Return Current (e.g., Stramma, 1989; Peterson and Stramma, 1991; Boebel et al., 1997). Other possible causes could be the location of the confluence of the Brazil Current and the Malvinas Current or the mesoscale variability in the confluence region (e.g., Gordon, 1989; Garzoli, 1993; Maamaatuaiahutapu et al., 1998). The separation of the Brazil Current Front from the shelf break can be used as a proxy to track changes in the location of the confluence (e.g., Goni et al., 2011), who showed a time series indicating that this separation typically occurs in 34.5 to 40.5^{o}S). The method for detecting the separation described in Goni et al. (2011) was used herein to determine if its location is correlated to the transport of the Brazil Current. No such correlation was found (not shown). Therefore, the most likely reason for the large fluctuation is the strong mesoscale variability in this region as indicated by the high eddy kinetic energy (e.g., Oliveira et al., 2009), their figure 6). Consistent with this, both the velocity field from Argo & SSH and HYCOM have relatively high eddy kinetic energy in the region most impacted by the Brazil Malvinas Confluence (from 33^{o}S on southward within about 15^o from the western boundary), when compared with the boundary region north of the confluence (not shown).

The standard deviations in Figure 4 tend to increase from north to south in observation-based and model results and the highest values are found in the confluence region. Naturally, the transports from the eddy-resolving HYCOM model have larger standard deviations than those from Argo & SSH. A closer look at the variability, after removing the mesoscale signals in the time series, follows in the next section.

4 Temporal variability of the Brazil Current transport

In the following the full time series (Fig. 5) is analyzed in conjunction with the annual cycle derived from the anomalies of the transport (Fig. 6). The anomalies have been derived by subtracting the annual mean for each year from the individual monthly transports in that year.

4.1 Variability at 24^{o}S

The transport from Argo & SSH in the upper 400 m at 24^{o}S ranges from 0.4 Sv to 4.8 Sv with a mean of 2.2±0.9 Sv (Table 2), and reveals a relatively complicated variability, mostly with one to two transport maxima in each year (black line, Fig. 5, top). Typically, the transports are high in austral summer and low in austral winter. This can be seen more clearly in Figure 6 (black line), which shows the annual cycle represented as the anomaly of the transport. On average, the smallest transport occurs in July and the largest in March. The amplitude of the annual cycle is 0.6 Sv, with transports ranging from 1.7 Sv to 2.8 Sv (Table 3). The years for which a semiannual cycle is indicated by two transport maxima give rise to the dip of the anomaly to about 0.1 Sv in October. However, in terms of indicating the presence of a semi-annual cycle this feature does not reach the level of significance. The alternating multi-year phases with significant spectral density at semi-annual and/or annual periods is reflected in the wavelet power spectrum (Fig. 7a). Longer-periodic variability also has relatively high spectral density, primarily for periods of 2 to 4 years, that almost reach the level of significance.

On average the Brazil Current transports from HYCOM are about 4 Sv larger than those from Argo & SSH, with a mean of 6.2±1.6 Sv and a range of 2.7 to 10.9 Sv (Table 2). With respect to the annual cycle, Figure 6 (red line) reveals two maxima (February and September) and two minima (June and December) at this latitude. All of these are within a month of the extreme values identified in the Argo & SSH record. It is noted, that the annual cycle from HYCOM and Argo & SSH are very similar from November until April, whereas the transport in HYCOM drops to a lower value in austral winter and then increases more sharply in June to September. Consequently, the amplitude of the annual cycle of 0.9 Sv is 50% larger than that for Argo & SSH (Table 3). The characteristics detected in the anomalies of the transport from HYCOM are in good agreement with the wavelet spectrum for this time series (not shown).

4.2 Variability at 35^{o}S

The meridional transports of the Brazil Current at 35^{o}S in the upper 800 m from Argo & SSH are in the range of 7.9 to 26.2 Sv with a mean of 16.5±3.2 Sv (Table 2, black line in middle panel of Fig. 5). The HYCOM time series has larger transports and variability (red line in middle panel of Fig. 5) which yields a larger mean and standard deviation (Table 2). As for 24^{o}S, some years in the Argo & SSH time series have two maxima of the transport while other years have only one. Figure 6 (black line) exhibits the transport minimum in June and the maximum in December. While the amplitude of 1.2 Sv is twice as large as at 24^{o}S the standard error is about four times larger (Table 3). The standard error in Figure 6 indicates that there is no significant mean semiannual or annual cycle at 35^{o}S. Consistent with this, the wavelet power spectrum of the transports reveals significant powers at 3 to 9 month time scales with relatively rare phases governed by a period of 6 months and no phases with a period of 12 months that reach the level of significance (Fig. 8a). However, in about 2000 to 2011, the power almost reaches the level of significance at the annual period. Phases with relatively high spectral density at periods of 2 years or more can be seen in Figure 8a, however, they are less significant than at 24^{o}S.

A transport time series for the Brazil Current derived sea surface height anomalies by Goni and Wainer (2001) and Goni et al. (2011) also indicated that the interannual variability and mesoscale variability are very strong which will make it hard to detect any annual cycle in observations that might exist. Goni et al. (2011) found a significant peak in a spectral analysis at the annual period and their time series has the relative minimum (maximum) of the transport occurred in austral winter (summer) in for four of the six years (Figure 7 of Goni et al., 2011) maxima are in general agreement with those found in the Argo & SSH time series.

In contrast to Argo & SSH, HYCOM has a significant annual cycle with an amplitude that is about three times larger than the amplitude from Argo & SSH (Fig. 6, middle). The good agreement in the timing of the maxima and minima detected in Argo & SSH as well as HYCOM indicates that a significant annual cycle might exist in the ocean but can not be resolved with observations. It is noted here, that the wavelet spectrum from HYCOM reveals a significant signal at the annual period in 2001 to 2013 (not shown), which is similar to the time frame of an almost significant annual cycle in the wavelet analysis for Argo & SSH mentioned in the previous paragraph. A likely reason for the weak signal at the annual time scale in Argo & SSH, when compared with HYCOM, could be due to insufficient in situ observations in this region with relatively large mesoscale variability (e.g., Oliveira et al., 2009). An indication that Argo & SSH might be undersampling the variability in this region is that the eddy kinetic energy in Argo & SSH at 35^{o}S is between one fifth and a quarter of the eddy kinetic energy in HYCOM (not shown). This suggests that undersampling with insitu observations could reduce the ability of Argo & SSH with respect to fully resolving the annual cycle.

4.3 Variability at 38^{o}S

At 38^{o}S, the transport in the upper 800 m from Argo & SSH cover a wider range of values than at 35^{o}S: 6.2 to 33.4 Sv, with a mean of 20.7$\pm$4.8 Sv (Table 2; black line in bottom panel of, Fig. 5). With respect to the mean annual cycle, the amplitude at 38^{o}S for Argo & SSH is the same as at 35^{o}S (1.2 Sv, Table 3) while the standard errors are larger (2.2 Sv versus 1.3 Sv for the monthly anomalies). While Figure 6 indicates that there is no significant mean annual or semi-annual cycle on average, the wavelet power spectrum of the Brazil Current transport from Argo & SSH (Fig. 8c) reveals phases with significant semi-annual and annual cycles. The latter dominates in the sense that it has a strong signal in 1999-2002 and 2007-2013. The annual cycle from HYCOM agrees well with Argo & SSH with respect to the timing (Fig. 6). In addition, the amplitude from HYCOM is closer to that from Argo & SSH than at 35^{o}S. This similarity is supported by the wavelet analysis for HYCOM (not shown) which reveals periods with a significant annual cycle that match those from Argo & SSH. At periods of 2 to 4 years the spectral density for Argo & SSH is larger than at 35^{o}S and smaller than at 24^{o}S.

Probably, a main reason for the absence of a clear mean annual cycle is the high variability associated with the confluence of the Brazil Current and Malvinas Current (e.g., Matano, 1993; Goni and Wainer, 2001). Similar to the situation at 35°S, the potential for undersampling could play a role at 38°S as well. However, the eddy kinetic energy from Argo & SSH is closer to that from HYCOM (reaching between 35 and 45% of the eddy kinetic energy in HYCOM, not shown). Therefore, the issue with undersampling the mesoscale variability might be less significant at 38°S. The location of the confluence is likely to play an important role here. As mentioned in section 3, Goni et al. (2011) reported that the Brazil Current Front, which can be used to trace the confluence, was between 34.5°S and 40.5°S in 1993 to 2008. On average it was near 38°S, which is the latitude discussed here.

According to Vivier and Provost (1999) the annual migrations of the Brazil Current Front are predominantly determined by the strength of the Brazil Current which is mainly forced by the local wind stress curl (Vivier et al., 2001). Similarly, Goni and Wainer (2001) came to the conclusion that the combination of changes of the transports of the Brazil Current and the Malvinas Current drive the migration of the Brazil Current Front and that the former has a larger influence than the latter. With respect to long-term trends of the Brazil Current Front Goni et al. (2011) suggested that transport changes of the Brazil Current and the Malvinas Current are not important for frontal migrations over the time period of about 15 years.

Spadone and Provost (2009) showed that the Malvinas Current has the highest transports in May to August near 40°S. During this season, the mean annual cycle indicates that the Brazil Current has relatively small transports at 38°S. The wavelet transform amplitude for the Malvinas Current near 40°S presented by Spadone and Provost (2009), which overlaps with the time series presented herein, has no similarity in terms of annual or semi-annual signals with the wavelet transform amplitude derived for the Brazil Current transport at 38°S. This is in agreement with the argument above that the frontal location is determined by the wind stress curl rather than the transports of these two currents.

4.4 Relationship to Ocean Indices

In an expansion of the analysis the interannual variability of the Brazil Current transport is studied. It is found that the differences of the transports between adjacent phases with high and low values are about 1 Sv at 24^{o}S and 2 to 3 Sv at 35^{o}S (Table 2). Typically, the time between two relatively low or high transports is in the range of 2 to 4 years. In addition, the transport at 24^{o}S increases, on average, over a six year time period (1994-2000), dips to a low point in 2002 from which it recovers quite rapidly (Fig. 9c). Another dip occurs in 2010.

In order to better understand what drives this variability, the relationship between various ocean indices (SAM, Niño 3.4 and AMO, see section 2) and the transport at 24^{o}S is investigated. Correlations between SAM and the transport of the Brazil Current are estimated for time series filtered with different cut-off periods. When filtering with cut-off periods of 6 to 18 months, the derived correlation coefficients are 0.5 with time lags of 6 to 7 months, depending on the applied filtering (Fig. 9, Table 4). Filtering less strongly (2 month cut-off period) yields a lower correlation and filtering more strongly (24 month cut-off period) results in a shift towards a lag of 9 months. While all of these correlations are significant with respect to the a 95% confidence level (estimated correlations that do not reach the level of significance are excluded from Table 4), the most robust estimate is the correlation of 0.5 with a 6 month lag. In agreement with this, the largest minima (maxima) of SAM are typically followed by minima (maxima) of the Brazil Current transport.

A similar analysis for the Niño 3.4 index yields a significant correlation of 0.4 to 0.5 with a lag of 8 months for the time series filtered with a 6 month or 12 month cut-off period. This lag is larger than the corresponding lag derived for SAM, which is not surprising since any teleconnections between the tropical Pacific and the subtropical South Atlantic can be expected to take more time than the dynamic impact of SAM on the subtropical South Atlantic. When looking in more detail at the time series (black and blue lines in Fig. 9), it is noted that the 1997/1998 El Niño was followed be a low transport of the Brazil Current. The Brazil Current transport also decreased after the peak of the El Niño conditions in 2002/2003 and 2009/2010. It is too early to be sure, but it seems like the strong El Niño of 2015/2016 could be followed by another dip in the transport of the Brazil Current. Similarly, several phases with La Nina conditions are followed by relatively high transports of the Brazil Current. In the next section, the analysis on the role that SAM and ENSO play with respect to forcing the variability of the Brazil Current transport is expanded.

For the AMO index, the correlations are less robust with a smaller correlation coefficients ranging from 0.3 to 0.4 and a wider range of lags encompassing 1 to 5 months. While most of these correlations with AMO reach the level of significance, the result is not considered to be robust due to the large range of lags (because of this, the AMO is not shown in Fig. 9). This is not very surprising, because the AMO is an index based on the conditions in the North Atlantic.

At 35^{o}S and 38^{o}S, the correlations are smaller and mostly have lags that agree well with those at 24^{o}S. Table 4 only contains few estimates for these latitudes because most of them were not significant. This is again, indicative for the importance of mesoscale variability in the vicinity of the Brazil Malvinas confluence.

4.5 Relationship between sea level pressure and meridional transport

A coupled EOF analysis of the anomalies of the sea level pressure (SLP) in a large region, including the Southern and tropical Atlantic and Pacific, and the meridional transport in the upper 800 m in the western South Atlantic (60 to 30^{o}W, 40 to 20^{o}S, which includes the Brazil Current) is performed to understand their covariability. The details on this method can be found, for example, in Bretherton et al. (1992). The use of a bigger domain for SLP is useful to understand large scale forcing and to assess the possibility of any teleconnection pattern (Wallace et al., 1992). The coupled EOF method used herein is widely used in climate studies to identify coupled patterns between two fields.

Figure 10 shows the heterogeneous and homogenous correlation maps (panels a, c) and the temporal expansion coefficients (panel b) for the first mode. This mode explains 36% of the variance. The spatial pattern of the heterogeneous correlation (Fig. 10a) reveals a quite strong zonal symmetry throughout the South Pacific and Atlantic, with the exception of the region south of South Africa and the tropics. South of the center of the subtropical gyres this pattern is associated with SAM, both in the Atlantic and the Pacific. In addition, the structure in the Atlantic reflects the variability in the subtropical gyre, with larger correlations near 40^{o}S in the region dominated by the Brazil Malvinas confluence and the South Atlantic Current as well as in the region where the southern South Equatorial Current is found. High correlations are also present in the western tropical Pacific, which are most likely due to teleconnections (e.g., Mo and Ghil, 1986; Lopez et al., 2016). This can be seen as a response of the southern hemisphere to El Niño Southern Oscillation (ENSO, Karoly, 1989) This spatial pattern is robust in the sense that it does not depend significantly on the filtering. The main impact of varying the filtering is that the variance explained as well as the correlation associated with ENSO decreases with decreasing cut-off period (not shown). This is not surprising because remote signals loose their strength as they propagate over long distances. Therefore, local forcing plays a more important role for short term variability than for long term variability. The spatial pattern of the homogeneous correlation (Fig. 10c) has the largest correlations in the region dominated by the Brazil Current.

The time series of the temporal expansions reveals alternating multi-year phases of relatively low and relatively high anomalies for the transport and the sea level pressure (Fig. 10b). Superimposed on this signal is some higher-frequency variability of varying amplitude. Similar characteristics are present in the time series of SAM (red line in Fig. 9b). The correlation of 0.7 between the temporal expansions is significant with respect to the 95% confidence level. Getting back to the role of ENSO, one can see large anomalies about half a year after the three strongest El Niño events during the studied time period (1997/1998, 2002/2003, 2009/2010, blue line in Fig. 9a), both for the sea level pressure and the transport (Fig. 10b). For SAM, the most prominent peaks are in 1993, 1999/2000, 2001, 2010 and 2015 (red line in Fig. 9a). Three of them are close to El Niño events (2001, 2010, 2015). In the temporal expansions, the two earlier ones can be associated with relatively large anomalies for the transport (Fig. 10b). For example, the 2009/2010 El Niño gives rise to an increase of the transport. As the El Niño weakens SAM becomes stronger which prevents a drop-off of the transport and, in fact, yields an additional increase of the transport. Similarly, the strong peak of SAM in 1999/2000, 2 years after a very strong El Niño terminates a reduction of the transport and gives rise to a secondary peak of the transport anomaly. One can conclude that SAM and El Niño together are important factors determining the interannual variability of the Brazil Current transport. How this works is described in the following.

The impact of SAM on the transport of the Brazil Current can be understood as follows. During periods of positive SAM, the westerly winds are stronger because of a more strongly developed low pressure system centered near 50^{o}S which gives rise to a relatively strong South Atlantic Current. Simultaneously, the subtropical high is stronger during the positive phase of SAM which results in easterly surface wind anomalies (Thompson and Wallace, 2000). This results in a strengthened subtropical gyre and thus a stronger western boundary current, in this case the Brazil Current. In an expansion of this argument,

Lopez et al. (2016) suggested that atmospheric Rossby waves originating in the tropical Pacific can travel south-eastward and reach the South Atlantic near the Drake Passage. These waves influence the sea level pressure in that region by giving rise to a low pressure anomaly centered at 50^{o}S which has an impact on the SAM index. The relationship between the Brazil Current transport from Argo & SSH and El Niño as well as SAM found herein is consistent with the mechanism proposed by Lopez et al. (2016). A more detailed discussion on the teleconnection pattern is beyond the scope of this manuscript.

Ocean Sci. Discuss., https://doi.org/10.5194/os-2017-59
Manuscript under review for journal Ocean Sci.
Discussion started: 4 August 2017

5 Summary and Conclusions

The analysis of a three-dimensional field of the horizontal velocity derived from observations covering 1993 to 2015 as well as velocity fields from HYCOM expands the knowledge of the spatial and temporal variability of the transport in the Brazil Current.

Consistent with previous studies, it is found that the mean transport of the Brazil Current as derived from Argo & SSH varies significantly with latitude, with smaller transports in the north (1.9±0.8 Sv in 20^{o}S to 25^{o}S), where this current originates and larger transports in the south near the confluence region (17.3±3.5 Sv in 33^{o}S to 39^{o}S). Between 25^{o}S and 32^{o}S, the transport from Argo & SSH increases gradually with a slope of 1.4±0.4 Sv per degree. This increase is primarily due to westward transports of the southern South Equatorial Current that reaches the western boundary largely within this latitude range. In principle, this is consistent with the Sverdrup balance. Farther south, the transport varies quite strongly from latitude to latitude, with an overall tendency to increase. This can be attributed to the Brazil Return Current that feeds water back into the Brazil Current as well as the Brazil-Malvinas confluence.

The observations reveal an annual cycle with a transport maximum in austral summer and a transport minimum in austral winter at 24^{o}S, 35^{o}S, and 38^{o}S (Figs. 5 and 6). However, it is found that the significance of the mean annual cycle decreases with increasing latitude (Fig. 6). A wavelet analysis indicates that phases of an annual cycle exist at all three latitudes, but their prevalence decreases with increasing latitude (Figs. 7 and 8). In agreement with this, the time series (Fig. 5) also reveals strong interannual variability, both in terms of shifts in the annual mean and in the timing of the highest and lowest transports.

With respect to the interannual variability it is found that the meridional transport of the Brazil Current switches from relatively high to relatively low values roughly every two to four years in the time series from Argo & SSH that were smoothed with a one year low-pass filter (Fig. 9b). The power spectrum from the cross wavelet transform at 24^{o}S shows weak signs for the presence of such variability that mostly do not quite reach the level of significance (Fig. 7c).

Time series smoothed with a filter using a 6 to 12 month cut-off period reveal a correlation of the Brazil Current transport with SAM that is within the 95% confidence interval with a lag of 6 months at 24^{o}S (section 4.4, Table 4). For the Niño 3.4 index the correlations with the transport remain significant while being slightly smaller with a larger lag of 8 months. The correlations between the transport and the AMO index are even smaller and the lags are not robust. These results are not surprising, because cross-hemispheric correlations (for AMO) or larger distances (for Niño 3.4) can be expected to result in a weaker influence.

The first mode of the coupled EOF between the meridional transport in the Brazil Current region and the sea level pressure provides insight with respect to the atmospheric forcing. It explains 36% of the variance and supports the influence of SAM and ENSO on the meridional transport (Fig. 10, section 4.5).

Data availability. The Argo & SSH velocity fields and transport estimates for this study will be made available online via http://www.aoml.noaa.gov/phod/argo/argo_and_science.php. Until that is accomplished, the data will be made available upon request to the corresponding author.

Competing interests. none

Acknowledgements. This paper was in part funded by the Climate Observation Division, Climate Program Office, National Oceanic and Atmospheric Administration (NOAA), U.S. Department of Commerce and the Atlantic Oceanographic and Meteorological Laboratory of the National Oceanic and Atmospheric Administration. This research was also carried out in part under the auspices of the Cooperative Institute for Marine and Atmospheric Studies (CIMAS), a cooperative institute of the University of Miami and the National Oceanic and Atmospheric Administration, cooperative agreement NA10OAR432013. The authors would like to thank the researchers and technicians involved in the Argo project for their contributions to generating a high-quality global sub-surface data set.

Argo data were obtained from a Global Data Assembly Centre (Argo GDAC, doi: 10.17882/42182). Altimeter products were produced by Ssalto/Duacs and distributed by AVISO, with support from Cnes (www.aviso.altimetry.fr/ducas/). Funding for the development of HYCOM has been provided by the National Ocean Partnership Program and the Office of Naval Research. Data assimilative products using HYCOM are funded by the U.S. Navy. Computer time was made available by the DOD High performance Computing Modernization Program. The output is publicly available at hycom.org. The velocity product derived from surface drifters is available at www.aoml.noaa.gov/phod/dac/dac_meanvel.php. The Southern Annular Mode (SAM) index was obtained from www.nerc-bas.ac.uk//icd//gjma//sam.html. The Atlantic Multidecadal Oscillation and El Niño index were obtained from NOAA and can be found at http://www.esrl.noaa.gov/psd/data/timeseries/AMO/ and from http://www.esrl.noaa.gov/psd/data/climateindices/list/. The MERRA products are available at disc.sci.gsfc.nasa.gov/mdisc/data-holdings/merra/merra_products_nonjs.shtml).

References

AVISO: AVISO User Handbook for Merged TOPEX/POSEIDON products., CLS, ref.: AVI-NT-02-101, 1996.

Biló, T. C., da Silveira, I. C. A., Belo, W. C., de Castro, B., and Piola, A. R.: Methods for estimating the velocities of the Brazil Current in the pre-salt reservoir area off southeast Brazil (23^oS-26^oS)., Ocean Dynamics, 64, 1431–1446, doi: 10.1007/s10 236–014–0761–2, 2014.

Boebel, O., Schmid, C., and Zenk, W.: Flow and recirculation of Antarctic Intermediate Water across the Rio Grande Rise., J. Geophys. Res., 102, 20,967–20,986, 1997.

Bretherton, C. S., Smith, C., and Wallace, J. M.: An intercomparison of methods for finding coupled patterns in climate data, J. Climate, 5, 541–560, 1992.

Campos, E. J. D., Gonçalves, J. E., and Ikeda, Y.: Water mass characteristics and geostrophic circulation in the South Brazil Bight: Summer of 1991., J. Geophys. Res., 100, 18,537–18,550, 1995.

Chassignet, E. P., Smith, L. T., Halliwell, G. R., and Bleck, R.: North Atlantic simulation with the HYbrid Coordinate Ocean Model (HYCOM): Impact of the vertical coordinate choice, reference density, and thermobaricity., J. Phys. Oceanogr., 33, 2504–2526, 2003.

de Ruijter, W. P. M.: Asymptotic analysis of the Agulhas and Brazil Current systems., J. Phys. Oceanogr., 12, 361–373, 1982.

Enfield, D. B., Mestas-Nunez, A. M., and Trimble, P. J.: The Atlantic Multidecadal Oscillation and its Relationship to Rainfall and River Flows in the Continental U.S., Geophys. Res. Lett., 28, 2077–2080, doi: 10.1029/2000GL012 745, 2001.

Evans, D. L. and Signorini, S. R.: Vertical structure of the Brazil Current., Nature, 315, 48–50, 1985.

Evans, D. L., Signorini, S. R., and Miranda, L. B.: A note on the Transport of the Brazil Current., J. Phys. Oceanogr., 13, 32–1738, 1983.

Fisher, A.: The circulation and stratification of the Brazil Current., M. S. thesis, pp. 86, New York University, 1964.

Garfield, N.: The Brazil Current at subtropical latitudes., Ph.D. thesis, Univ. of Rhode Island, 1990.

Garzoli, S. L.: Geostrophic velocity and transport variability in the Brazil/Malvinas Confluence., Deep-Sea Res., 40, 1379–1404, 1993.

Garzoli, S. L. and Garraffo, Z.: Transports, frontal motions and eddies at the Brazil-Malvinas currents confluence., Deep-Sea Res., 36, 681–703, 1989.

Garzoli, S. L., Baringer, M. O., Dong, S., a, R. C. P., and Yao, Q.: South Atlantic meridional fluxes., Deep-Sea Res. I, 71, 21–32, doi: 10.1016/j.dsr.2012.09.003, 2013.

Goni, G. J. and Wainer, I.: Brazil Current front dynamics from altimeter data., J. Geophys. Res., 106, 31,117–31,128, 2001.

Goni, G. J., Bringas, F., and DiNezio, P. N.: Observed low frequency variability of the Brazil Current front., J. Geophys. Res., 116, 1–10, doi:10.1029/2011JC007 198, 2011.

Gordon, A. L.: Brazil-Malvinas Confluence - 1984., Deep-Sea Res., 36, 359–384, 1989.

Gordon, A. L. and Greengrove, L. C.: Geostrophic circulation of the Brazil-Falkland confluence., Deep-Sea Res., 33, 573–585, 1986.

Gordon, A. L., Weiss, R. F., Smethie, W. M., and Warner, M. J.: Thermocline and Intermediate Water communication between the South Atlantic and Indian Oceans., J. Geophys. Res., 97, 7223–7240, 1992.

Jullion, L., Heywood, K. J., Garabato, A. C. N., and Stevens, D. P.: Circulation and Water Mass Modification in the Brazil-Malvinas Confluence., J. Phys. Oceanogr., 40, 845–864, doi: 10.1175/2009JPO4174.1, 2006.

Kanamitsu, M., Ebisuzaki, W., Woollen, J., Yang, S.-K., Hnilo, J., Fiorino, M., and Potter, G. L.: NCEP-DEO AMIP-II Reanalysis (R-2)., Bull. Amer. Meteor. Soc., 83, 1631–1643, 2002.

Karoly, D. J.: Southern Hemisphere circulation features associated with El Niño-Southern Oscillation events., J. Climate, 2, 1239–1251, 1989.

Lima, M. O., M. Cirano and, M. M., Goes, M., Goni, G., and Baringer, M. O.: An assessment of the Brazil Current baroclinic structure and variability near 22^{o}S in distinct ocean forecasting and analysis systems., Ocean Dynamics, 66, 893 – 916, doi: 10.1007/s10 236–016–0959–6, 2016.

Lopez, H., Dong, S., Lee, S.-K., and Campos, E.: Remote influence of interdecadal Pacific Oscillation on the South Atlantic Meridional Overturning Circulation variability., Geophys. Res. Lett., 43, 8250–8258, doi:10.1002/2016GL069 067, 2016.

Luyten, J. R., Pedlosky, J., and Stommel, H. M.: The ventilated thermocline., J. Phys. Oceanogr., 13, 292–309, 1983.

Maamaatuaiahutapu, K., Garçon, V. C., Provost, C., and Mercier, H.: Transports of the Brazil and Malvinas Currents at their Confluence, J. Mar. Res., 56, 417–438, 1998.

Majumder, S., Schmid, C., and Halliwell, G.: An observations and model-based analysis of meridional transports in the South Atlantic, J. Geophys. Res., 121, doi: 10.1002/2016JC011 693, 2016.

Marshall, G. J.: Trends in the Southern Annular Mode from observations and reanalyses., J. Climate, 16, 4134–4143, 2003.

Mata, M. M., Cirano, M., van Caspe, M., Fonteles, C., Goni, G., and Baringer, M.: Observations of Brazil Current baroclinic transport near 22^{o}S: variability from the AX97 XBT transect., CLIVAR Exchanges, 58, 5–10, 2012.

Matano, R. P.: On the Separation of the Brazil Current from the Coast., J. Phys. Oceanogr., 23, 79–89, 1993.

Mill, G. N., da Costa, V. S., Lima, N. D., nd L. A. A. Guerra, M. G., and Paiva, A. M.: Northward migration of Cape São Tomé rings, Brazil., Cont. Shelf Res., 106, 27–37, doi: 10.1016/j.csr.2015.06.010, 2015.

Miranda, L. and Castro Filho, B. M.: Condições de movimento geostrófico das águas adjacentes a Cabo Frio (RJ)., Bolm Inst. oceanogr., S Paulo, 28, 79–93, 1979.

Miranda, L. and Castro Filho, B. M.: Geostrophic flow conditions of the Brazil Current at 19°S., Ciencia Interamerica, 22, 44–48, 1981.

Mo, K. C. and Ghil, M.: Statistics and dynamics of persistent anomalies, J. Atmos. Sci., 44, 877–901, 1986.

Msadek, R., Johns, W. E., Yeager, S. G., Danabasoglu, G., Delworth, T. L., and Rosatiglu, A.: The Atlantic Meridional Heat Transport at 26.58N and Its Relationship with the MOC in the RAPID Array and the GFDL and NCAR Coupled Models., J. Climate, 26, 4335–4356, doi: 10.1175/JCLI–D–12–00 081.1, 2014.

Müller, T., Ikeda, Y., Zangenberg, N., and Nonato, L.: Direct measurements of western boundary currents off Brazil between 20S and 28S., J. Geophys. Res., 103, 5429–5437, doi 10.1029/97JC03 529, 1998.

Oliveira, L. R., Piola, A. R., Mata, M. M., and Soares, I. D.: Brazil Current surface circulation and energetics observed from drifting buoys., J. Geophys. Res., 114, 1–12, doi:10.1029/2008JC004 900, 2009.

Peterson, R. G.: On the volume transport in the southwestern South Atlantic (abstract), EOS, Trans., Amer. Geophys. Union, 71, 542, 1990.

Peterson, R. G. and Stramma, L.: Upper-level circulation in the South Atlantic Ocean., Progress in Oceanography, 26, 1–73, 1991.

Pond, S. and Pickard, G.: Introductory Dynamical Oceanography., Pergamon Press, 1983.

Rienecker, M. M., Suarez, M. J., Gelaro, R., Todling, R., Bacmeister, J., Liu, E., Bosilovich, M. G., Schubert, S. D., Takacs, L., Kim, G.-K., Bloom, S., Chen, J., Collins, D., Conaty, A., and da Silva, A.: MERRA: NASA's Modern-Era Retrospective Analysis for Research and Applications., J. Climate, 24, 3624–3648, doi:10.1175/JCLI–D–11–00 015.1, 2011.

Rocha, C. B., Tandon, A., da Silveira, I. C. A., and Lima, J. A. M.: Traditional quasi-geostrophic modes and surface quasi-geostrophic solutions in the Southwestern Atlantic., J. Geophys. Res., 118, 2734–2745, doi:10.1002/jgrc.20 214, 2013.

Rocha, C. B., da Silveira, I. C. A., Castro, B. M., and Lima, J. A. M.: Vertical structure, energetics, and dynamics of the Brazil Current System at 22^{o}S-28^{o}S., J. Geophys. Res., 119, 52–69, doi:10.1002/2013JC009 143, 2014.

Schmid, C.: Mean vertical and horizontal structure of the subtropical circulation in the South Atlantic from three-dimensional observed velocity fields., Deep-Sea Res. I, 91, 50–71, doi: 10.1016/j.dsr.2014.04.015, 2014.

Schmid, C., Schäfer, H., Podestá, G., and Zenk, W.: The Vitória eddy and its relation to the Brazil Current., J. Phys. Oceanogr., 25, 2532–2546, 1995.

Schmid, C., Siedler, G., and Zenk, W.: Dynamics of Intermediate Water Circulation in the Subtropical South Atlantic., J. Phys. Oceanogr., 30, 3191–3211, 2000.

Signorini, S. R.: On the circulation and the volume transport of the Brazil Current between the Cape of Sào Tomé and Guanabara Bay., Deep-Sea Res., 25, 481–490, 1978.

Spadone, A. and Provost, C.: Variations in the Malvinas Current volume transport since October 1992., J. Geophys. Res., 114, 1–21, doi:10.1029/2008JC004 882, 2009.

Stramma, L.: The Brazil Current transport south of 23 S., Deep-Sea Res., 36, 639–646, 1989.

Stramma, L., Ikeda, Y., and Peterson, R. G.: Geostrophic transport in the Brazil Current region., Deep-Sea Res., 37, 1875–1886, 1990.

Thompson, D. W. J. and Wallace, J. M.: Annular Modes in the Extratropical Circulation. Part I: Month-to-Month Variability., J. Climate, 13, 1000–1016, 2000.

Trenberth, K. E.: The Definition of El Niño., Bull. Amer. Meteor. Soc., 78, 2771–2777, doi: 10.1175/1520–0477(1997)078, 1997.

Vivier, F. and Provost, C.: Direct velocity measurements in the Malvinas Current., J. Geophys. Res., 104, 21,083–21,103, 1999.

Vivier, F., Provost, C., and Meredith, M. P.: Remote and Local Forcing in the Brazil-Malvinas Region., J. Phys. Oceanogr., 31, 892–913, 2001.

Wallace, J. M., Smith, C., and Bretherton, C. S.: Singular value decomposition of wintertime sea surface temperature and 500-mb height anomalies, J. Climate, 5, 561–576, 1992.

Zemba, J. C.: The structure and transport of the Brazil Current between 27° and 36° south., Ph.D. thesis, Woods Hole Oceanographic Institution, 1991.

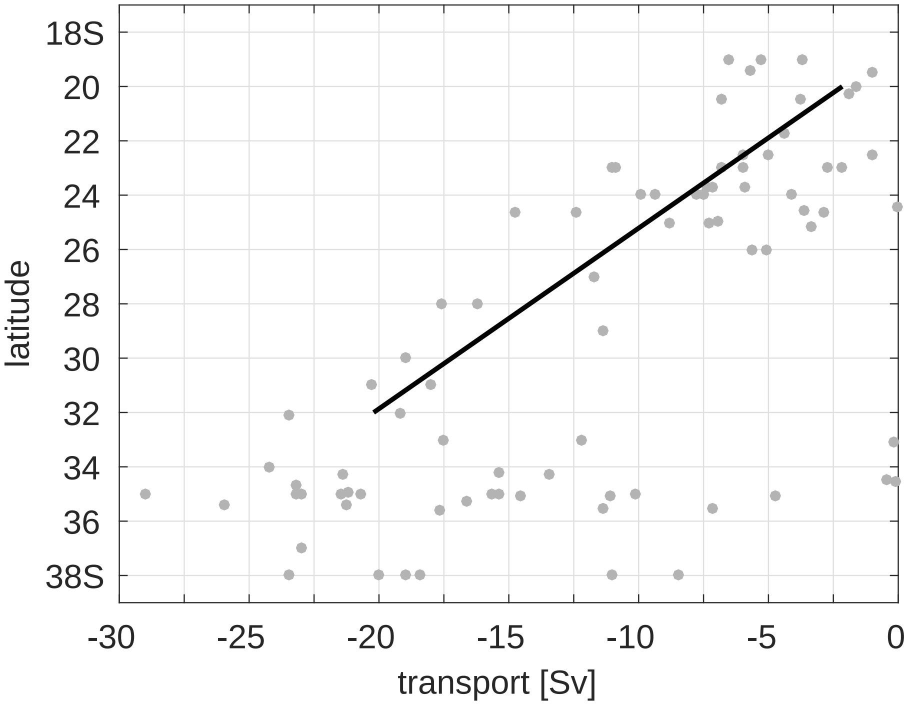

Figure 1. Previously published estimates of the Brazil Current transports as a function of latitude. The line with a slope of about 1.6 Sv per degree is a fit to the transports measured in 19^{o}S to 32^{o}S. The sources of the transport estimates are: Fisher (1964), Signorini (1978), Miranda and Castro Filho (1979), Miranda and Castro Filho (1981), Evans et al. (1983), Evans and Signorini (1985) Gordon and Greengrove (1986), Garzoli and Garraffo (1989), Gordon (1989), Stramma (1989), Garfield (1990), Peterson (1990), Stramma et al. (1990), Zemba (1991), Garzoli (1993), Campos et al. (1995), Maamaatuaiahutapu et al. (1998), Müller et al. (1998), Jullion et al. (2006), Mata et al. (2012), Garzoli et al. (2013) and Biló et al. (2014).

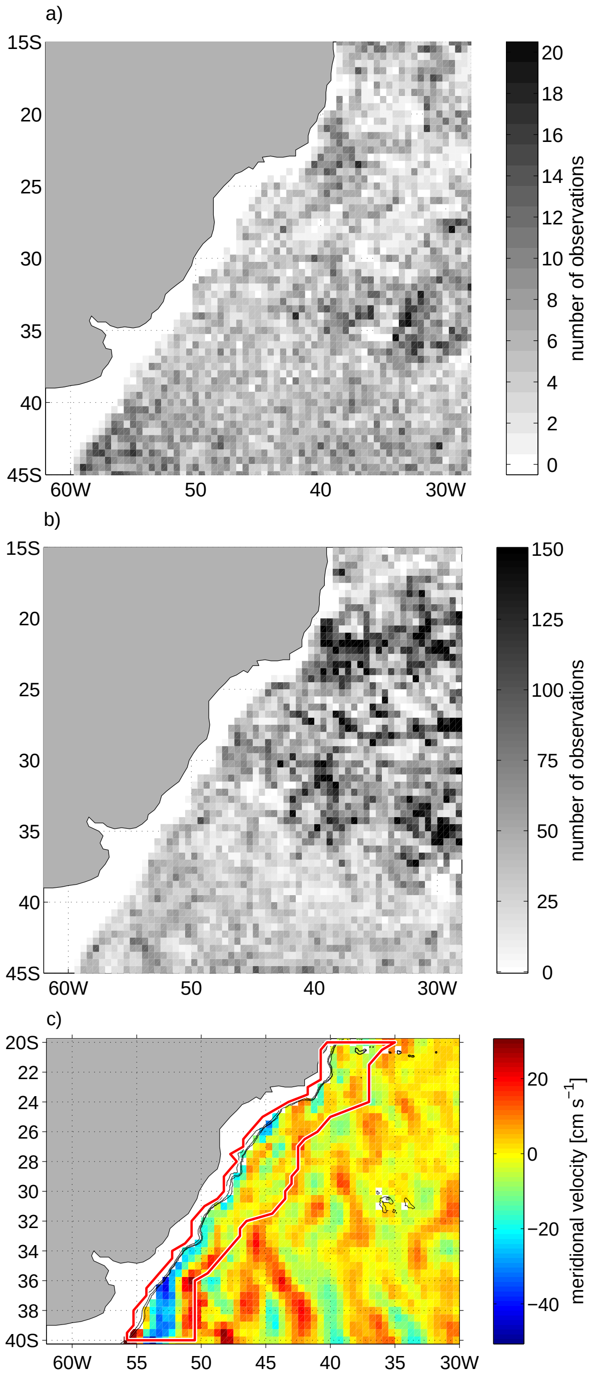

Figure 2. a) Availability of Argo profiles with temperature and salinity in the study region for observations collected in the years 2000 to 2015. b) Availability of trajectory observations in the study region for observations collected in January 9, 1992 to May 2, 2016. c) Meridional velocity in the surface layer from Argo & SSH for January 2015. The coastline as well as the 400, 800 and 1000 m isobaths are shown. The region encompassed by the red line indicates the search area for the southward flow of the Brazil Current. The bin sizes are 0.5^o by 0.5^o.

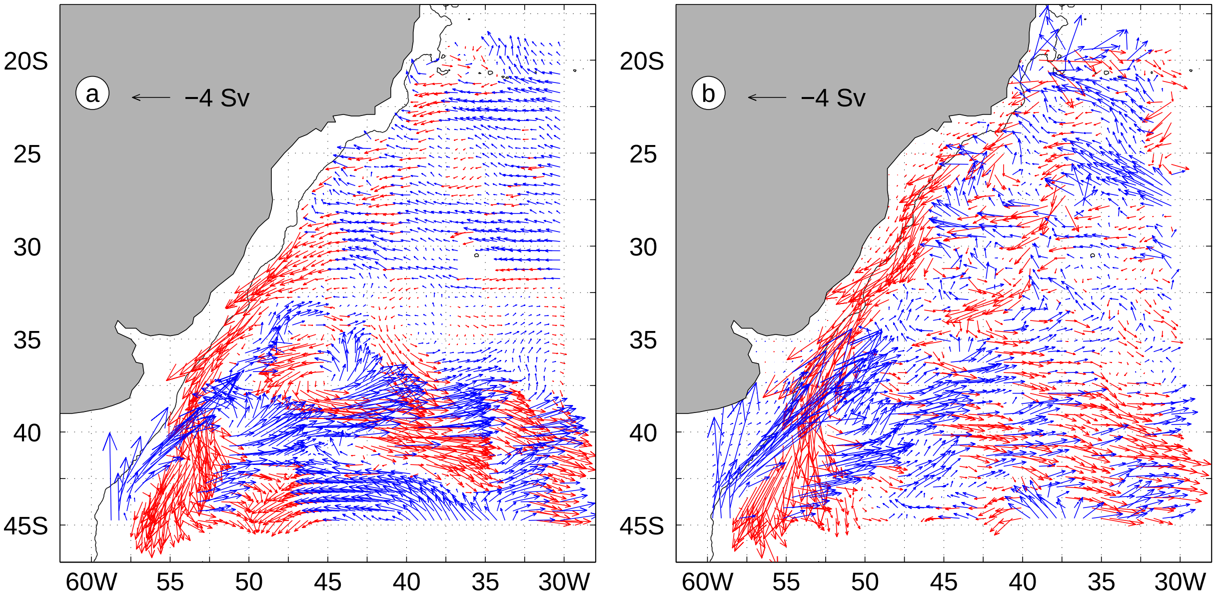

Figure 3. Climatological transport in the upper 800 m of the southwestern South Atlantic based on Argo & SSH (a), HYCOM (b). Red (blue) vectors indicate southward (northward) meridional transports. The 800 m bathymetry contour is also shown. It has to be noted that for HYCOM the resolution of 1/12^o has been reduced to match the resolution of Argo & SSH (0.5^o) for the sake of visibility and comparability of the vectors.

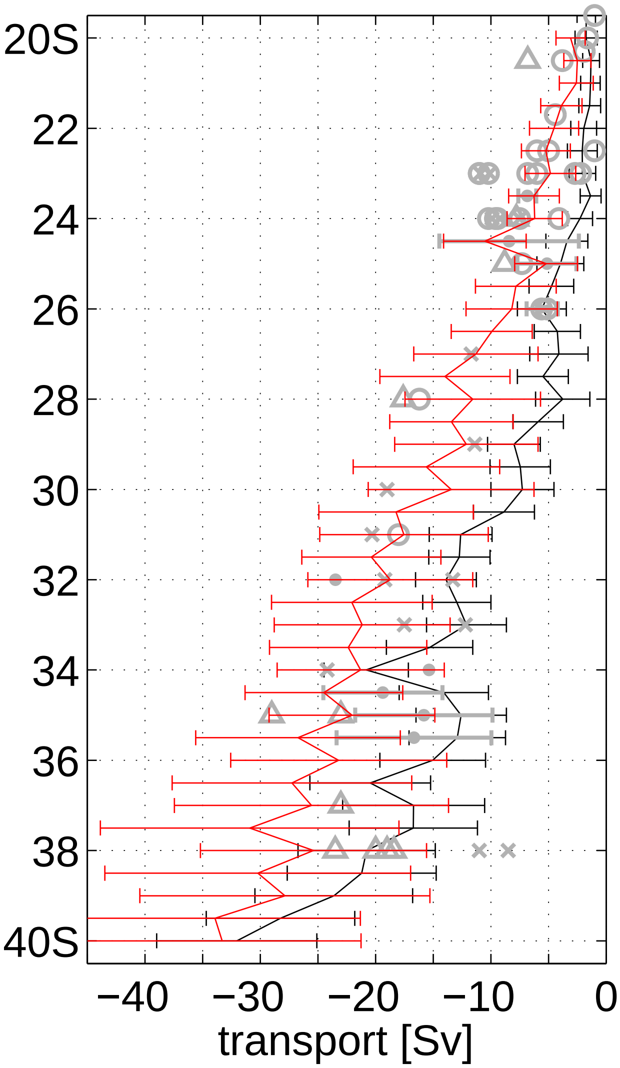

Figure 4. Climatological mean of the meridional transports of the Brazil Current as a function of latitude from observations (black, grey) and HYCOM (red). The black line with error bars shows the mean from Argo & SSH for a layer thickness of 400 m north of 27^{o}S and 800 m elsewhere. Gray symbols with or without error bars are from previous studies (see Figure 1 for references). The symbols indicate if the integration depth is less than 800 m (circles), 800 m (crosses and dots) or greater than 800 m (triangles). Gray error bars are shown if the estimate is from several transects or a time series. Gray dots are based on velocity transects derived by Garzoli et al. (2013) for the purpose of estimating the Meridional Overturning Circulation transports in the South Atlantic. The red line represents the mean with error bars as derived from a combination of the HYCOM reanalysis (1993-2012) and the HYCOM analysis (2013-2015). All error bars indicate the standard deviation associated with the mean.

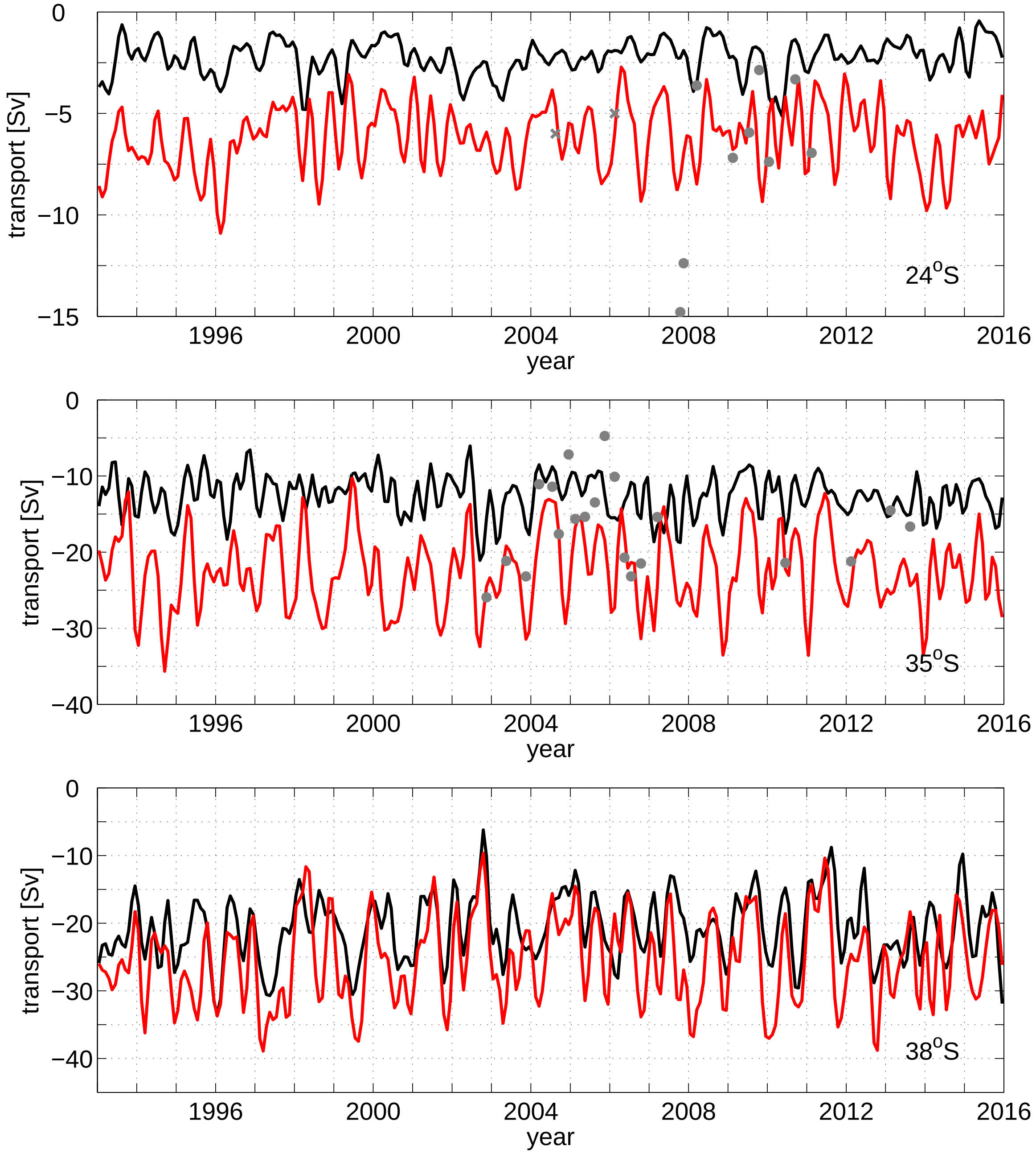

Figure 5. Time series of the meridional transports in the Brazil Current at 24^{o}S, 35^{o}S and 38^{o}S from Argo & SSH (black) and HYCOM (red). The depth range is 0 to 400 m at 24^{o}S and 0 to 800 m at the other latitudes. The time series were smoothed with a second order Butterworth filter (2 month low pass). Gray dots are based on transport estimates by Garzoli et al. (2013). Gray crosses indicate estimates from other studies (see Figure 1 for references).

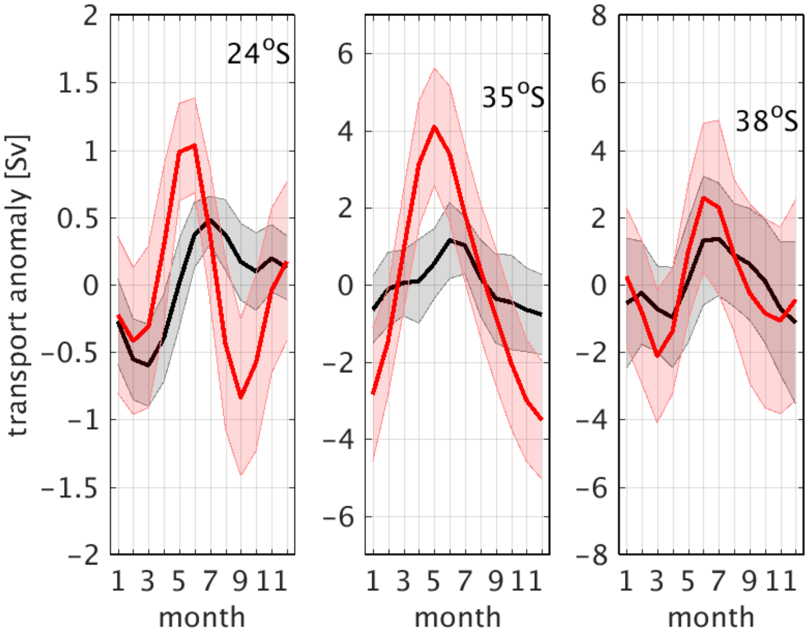

Figure 6. Annual cycle of the anomaly of the meridional transports in the Brazil Current derived from the time series in Figure 5 for 24^{o}S, 35^{o}S and 38^{o}S from Argo & SSH (black) and HYCOM (red). Shading indicates standard errors.

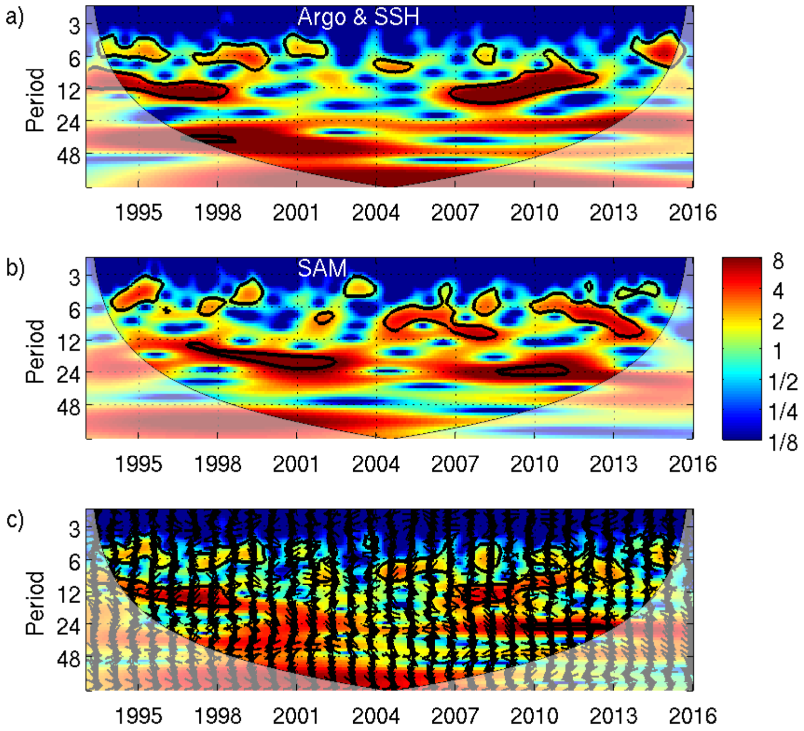

Figure 7. Wavelet power spectrum at 24^{o}S for Brazil Current transport from Argo & SSH (a) and SAM (b). (c) shows the cross wavelet power spectrum between the Brazil Current transport from Argo & SSH and SAM. The vectors in the lower panel indicate the phase difference between them. The thick black line is the 5% significance level using the red noise model, and the thin black line indicates the cone of influence. The time series were smoothed in the same way as the time series of the Brazil Current transport in Figure 5.

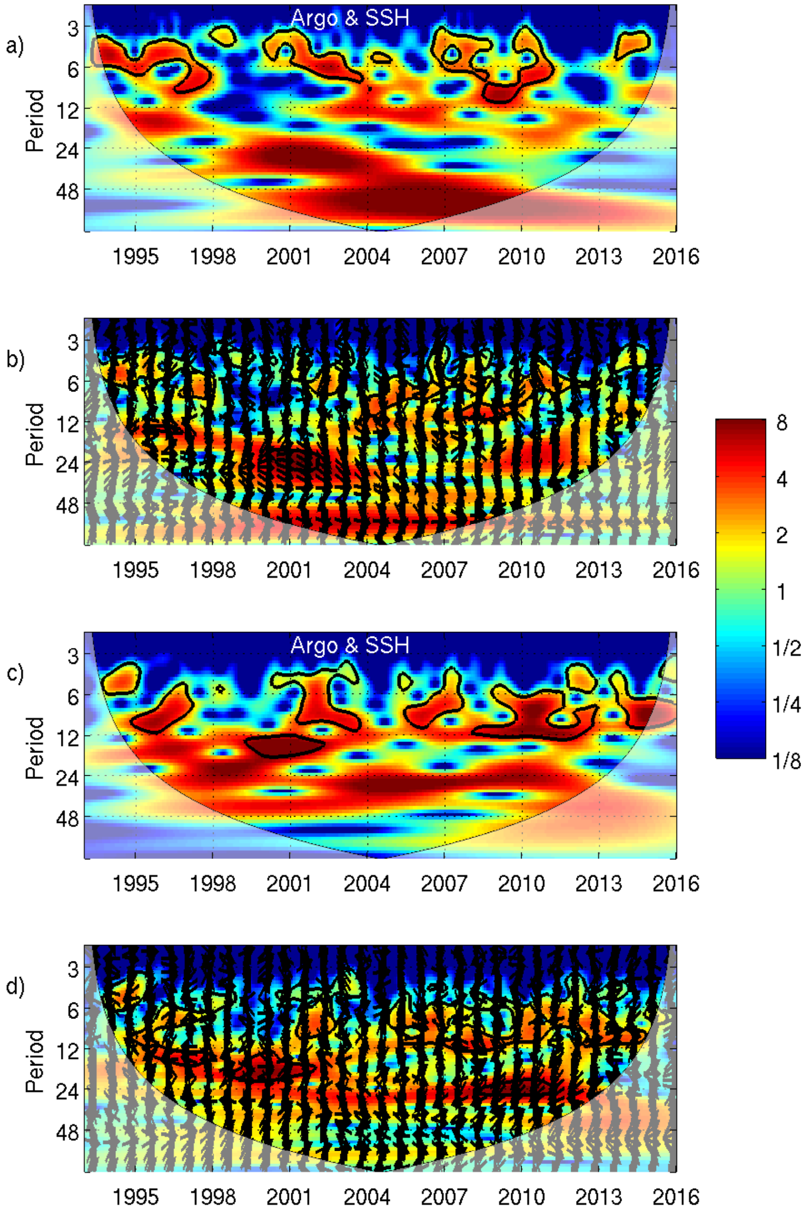

Figure 8. Wavelet power spectrum at 35°S (a, b) and 38°S (c, d) for Brazil Current transport from Argo & SSH (a, c). (b) and (d) show the cross wavelet power spectrum between SAM (Fig. 7b) and the Brazil Current transport from Argo & SSH for these two latitudes. The vectors in the lower panel indicate the phase difference between them. The thick black line is the 5% significance level using the red noise model, and the thin black line indicates the cone of influence. The time series were smoothed in the same way as the time series of the Brazil Current transport in Figure 5.

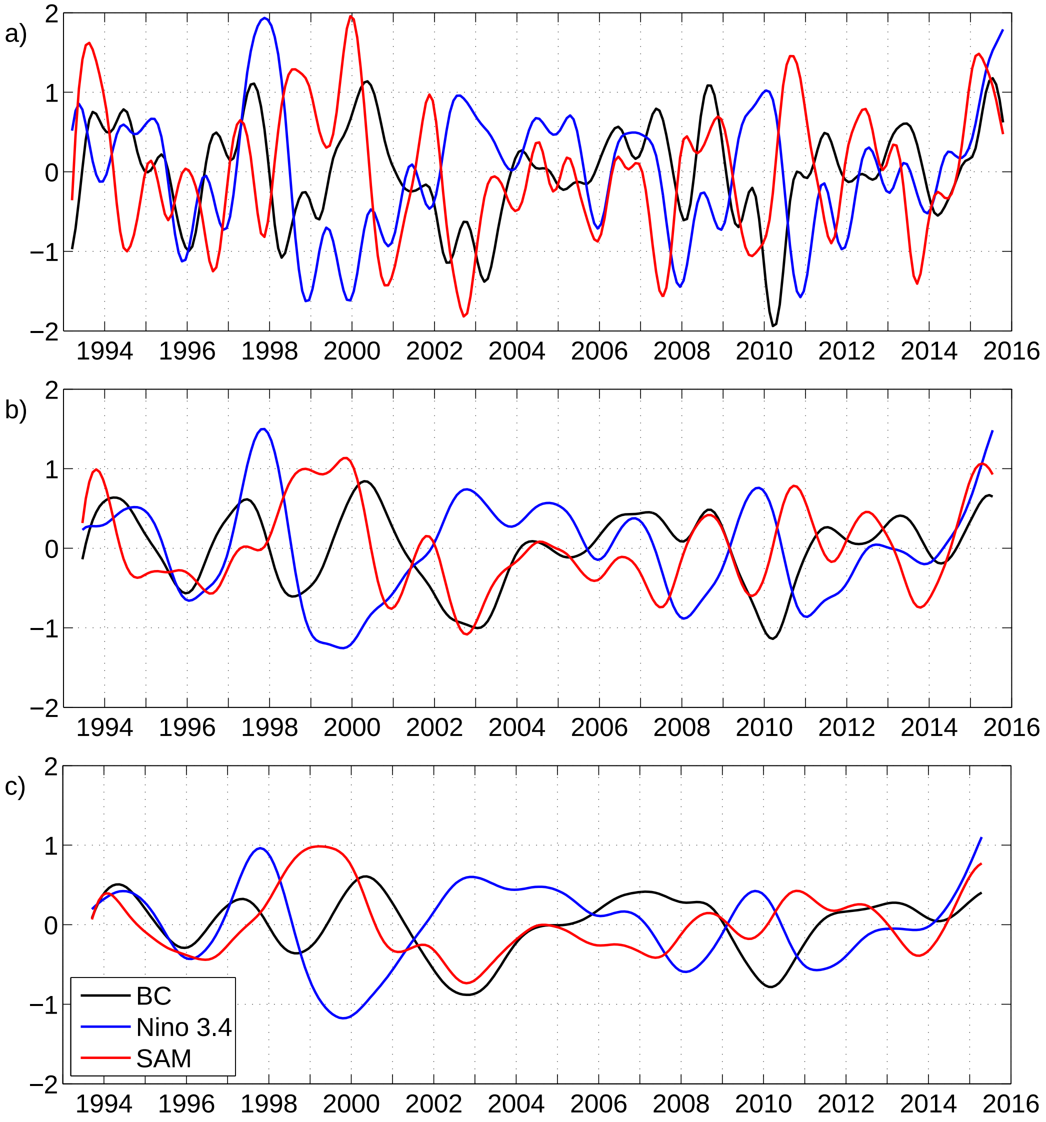

Figure 9. Southern Annular Mode (SAM) and Niño 3.4 index in comparison with meridional transports in the Brazil Current (BC) derived from the time series in Figure 5 for 24^{o}S. (a) smoothed with a 6 month Butterworth filter. (b) smoothed with a 12 month Butterworth filter. (c) smoothed with a 18 month Butterworth filter. The linear trend has been removed from all time series to allow the derivation of cross correlations. On average, the differences between these time series and the original ones are -2.2±0.1 Sv for the Brazil Current transports, 0.5±0.1 for SAM, and 27.1±0.1 for Niño 3.4.

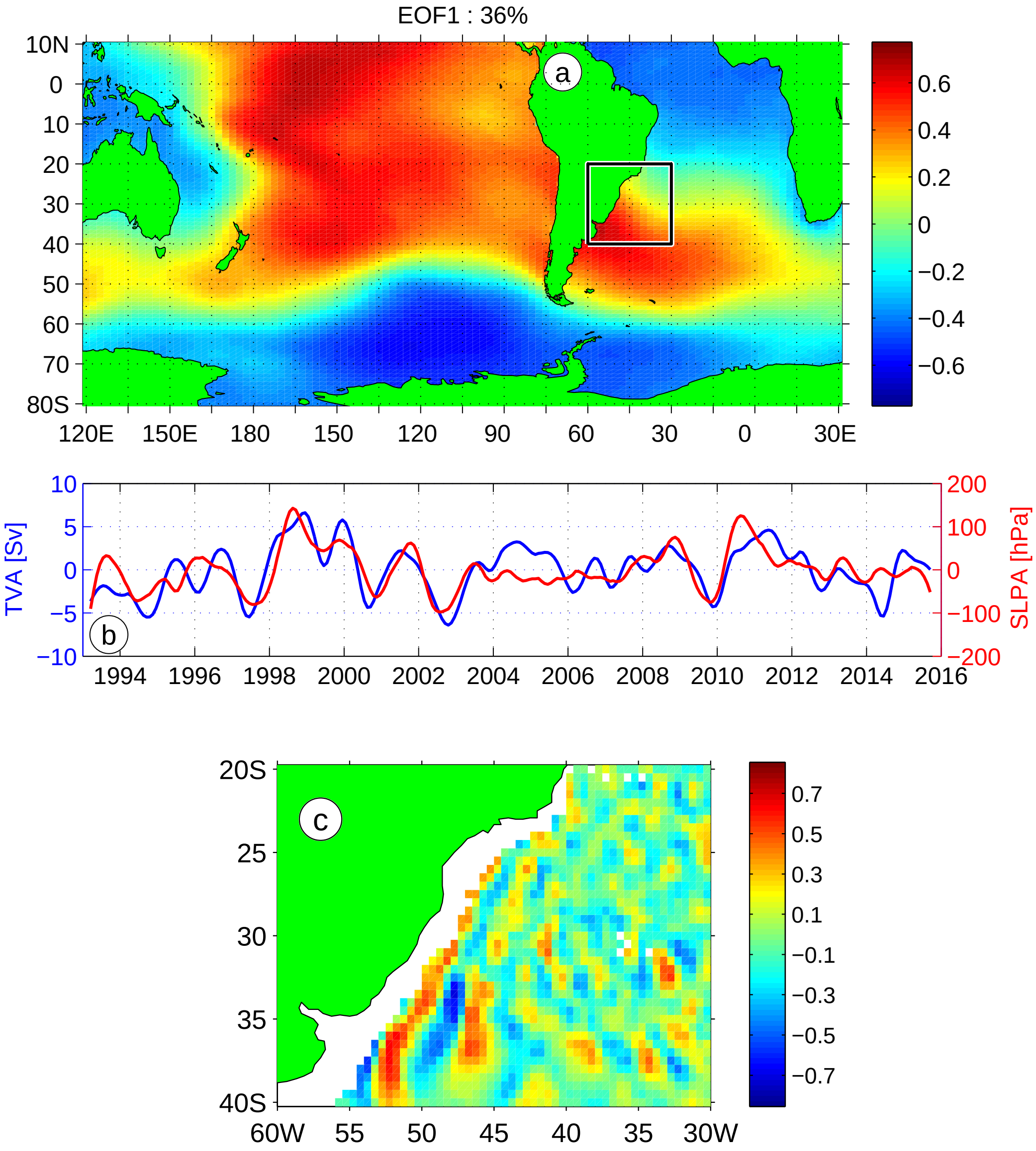

Figure 10. First mode of coupled EOF of the anomaly of the meridional transport (TVA) from Argo & SSH (in the box centered at 30^{o}S, 45^{o}W) and the anomaly of the sea level pressure (SLPA) from MERRA. The mean annual cycle was subtracted and the time series were filtered using a six month cut-off period. The spatial patterns of the heterogeneous correlation maps are presented in (a). The time series of the expansion coefficients (b) and the homogenous correlation (c) are shown as well. The correlation between the expansion coefficients is 0.7, which is significant with respect to the 95% confidence level. hPa = Hectopascal.

Table 1. Statistics of transports in the Brazil Current region from Argo & SSH and HYCOM in various layers for two latitude ranges.

Argo & SSH

latitude range	layer [m]	minimum [Sv]	maximum [Sv]	mean [Sv]	standard deviation [Sv]
20 - 27^{o}S	0-400	1.3	5.6	2.7	1.4
20 - 27^{o}S	0-800	1.5	7.0	3.3	1.8
33 - 39^{o}S	0-400	7.2	15.3	11.1	2.5
33 - 39^{o}S	0-800	12.1	23.3	17.3	3.5

HYCOM

latitude range	layer [m]	minimum [Sv]	maximum [Sv]	mean [Sv]	standard deviation [Sv]
20 - 27^{o}S	0-400	2.5	10.5	6.0	2.6
20 - 27^{o}S	0-800	3.1	13.1	7.2	3.2
33 - 39^{o}S	0-400	14.9	20.2	17.2	1.6
33 - 39^{o}S	0-800	21.2	30.9	25.3	3.2

Table 2. Statistics of transports of the Brazil Current from Argo & SSH for the whole time series as well as for periods of relatively low or relatively high transports. Estimates are derived from the time series in Figure 5.

Argo & SSH

period	latitude	median [Sv]	mean [Sv]	minimum [Sv]	maximum [Sv]	standard deviation [Sv]	standard error [Sv]
01/1993-12/2015	24°S	2.1	2.2	0.4	4.8	0.9	0.1
01/1993-12/2015	35°S	16.4	16.5	7.9	26.2	3.2	0.4
01/1993-12/2015	38°S	20.9	20.7	6.2	33.4	4.8	0.6
08/1993-12/1994	24°S	2.0	1.8	0.6	2.8	0.6	0.3
02/1995-04/1996	24°S	2.9	2.8	1.2	4.0	0.8	0.4
09/1996-11/2000	24°S	1.8	2.1	0.8	4.8	0.9	0.3
10/2000-11/2003	24°S	2.7	2.9	1.8	4.4	0.7	0.2
11/2005-10/2013	24°S	1.9	2.0	0.8	4.6	0.8	0.2
02/1995-08/1997	35°S	13.6	14.7	7.9	24.0	3.6	1.3
10/2003-10/2006	35°S	15.6	16.3	12.1	21.9	2.9	1.0
11/2005-08/2008	35°S	18.1	18.0	10.9	23.9	3.2	1.1
09/2008-06/2010	35°S	14.8	15.9	10.3	23.1	3.8	1.7
07/2011-01/2015	35°S	17.6	17.5	12.7	22.6	1.9	0.6

HYCOM

period	latitude	median [Sv]	mean [Sv]	minimum [Sv]	maximum [Sv]	standard deviation [Sv]	standard error [Sv]
01/1993-12/2015	24°S	6.1	6.2	2.7	10.9	1.6	0.2
01/1993-12/2015	35°S	22.5	22.5	10.2	35.6	5.0	0.6
01/1993-12/2015	38°S	25.4	25.5	9.6	38.9	6.4	0.8
08/1993-12/1994	24°S	6.9	6.7	4.7	8.3	1.0	0.5
02/1995-04/1996	24°S	7.9	8.0	5.2	10.9	1.7	1.0
09/1996-11/2000	24°S	5.5	5.7	3.1	9.5	1.4	0.4
10/2000-11/2003	24°S	6.4	6.4	3.2	8.7	1.3	0.4
11/2005-10/2013	24°S	5.7	5.9	2.7	9.4	1.6	0.3
02/1995-08/1997	35°S	22.2	21.8	13.9	29.6	3.9	1.4
10/2003-09/2006	35°S	19.9	20.7	13.1	31.4	5.3	1.8
10/2006-02/2009	35°S	24.6	24.1	14.0	33.5	5.0	1.9
03/2009-08/2012	35°S	20.1	20.5	12.3	33.6	5.0	1.6
09/2012-04/2014	35°S	24.2	24.5	18.3	33.5	3.5	1.6

Ocean Sci. Discuss., https://doi.org/10.5194/os-2017-59
Manuscript under review for journal Ocean Sci.
Discussion started: 4 August 2017

Table 3. Statistics and characteristics of the annual cycle of transports of the Brazil Current. Estimates are derived from the time series in Figure 5 (2001-2013 for Argo & SSH, see text and Fig. 6).

based on	amplitude [Sv]	standard error [Sv]	minimum [Sv]	maximum [Sv]
	24°S, 0-400 m, mean			
Argo & SSH	0.6	0.3	1.7	2.8
HYCOM	0.9	0.6	5.2	7.0
	24°S, 0-400 m, anomaly			
Argo & SSH	0.6	0.3	-0.6	0.5
HYCOM	0.9	0.6	-0.8	1.0
	35°S, 0-800 m, mean			
Argo & SSH	1.2	1.4	15.1	17.6
HYCOM	3.8	1.8	18.4	26.0
	35°S, 0-800 m, anomaly			
Argo & SSH	1.2	1.3	-1.1	1.4
HYCOM	3.8	1.7	-3.5	4.1
	38°S, 0-800 m, mean			
Argo & SSH	1.2	2.2	19.4	21.9
HYCOM	2.4	2.7	22.9	27.6
	38°S, 0-800 m, anomaly			
Argo & SSH	1.2	1.8	-1.2	1.3
HYCOM	2.4	2.2	-2.1	2.6

Table 4. Correlations between various indexes and the transport of Brazil Current (BCT). The filtered time series for the Brazil Current and Southern Annular Mode (SAM) are shown in Figure 9. AMO = Atlantic Multi-decadal Oscillation index, CL = confidence limit.

filter	correlation	lag	95% CL
BCT at 24^{o}S and SAM			
2 month	0.3	5	0.1
6 month	0.5	6	0.2
12 month	0.5	6	0.2
18 month	0.5	7	0.3
24 month	0.5	9	0.3
BCT at 24^{o}S and Niño 3.4 index			
2 month	0.4	9	0.2
6 month	0.4	8	0.2
12 month	0.5	8	0.2
18 month	0.4	6	0.2
24 month	0.5	2	0.3
BCT at 24^{o}S and AMO			
2 month	0.3	5	0.1
6 month	0.3	4	0.2
12 month	0.4	1	0.1
18 month	0.3	3	0.3
BCT at 35^{o}S and SAM			
2 month	0.2	5	0.1
6 month	0.3	3	0.2
BCT at 38^{o}S and Niño 3.4 index			
6 month	0.2	8	0.1

Appendix A: Details on how the Brazil Current transport is estimated

Transport profiles in grid boxes that have a water depth of less than 1000 m in their center are excluded. This means that at most latitudes, the Argo & SSH data set has a profile of the transport within less than 0.25^o of the 600 m isobath. The search area for the Brazil Current is indicated by the red line in Figure 2c that encompasses the region near the shelf break where this current is typically found. It extends east of the climatological mean core of the Brazil Current to allow for its meandering. The procedure is to pick the westernmost southward current for estimating the transport unless it is not part of the continuous southward flow. The latter situation is mostly encountered in the northern part of the domain, where a single grid box with southward velocity might exist at the shelf break while the boxes south and north of it do not support treating this box as part of the Brazil Current. An example of a situation like this near 20^{o}S was studied by Schmid et al. (1995). Many others also looked at the zonal position of this current (some recent studies on this topic are (Biló et al., 2014; Mill et al., 2015; Lima et al., 2016). The Brazil Current transports are derived by integrating the meridional velocity within the identified longitude range at each latitude.

Appendix B: Quantifying uncertainties of the Brazil Current transport

Previous studies showed that the velocity field from Argo & SSH reproduces the features of the circulation in the South Atlantic (Schmid, 2014) and can be used to derive the integrated transports associated with the Meridional Overturning Circulation at multiple latitudes (Majumder et al., 2016). Because Argo & SSH is used herein to study the variability of the transport in the Brazil Current it is important to know what uncertainties exist. Quasi-synoptic XBT transects as well as output from the HYCOM model are used to quantify the contribution of transports in shallow water to the total transport of the Brazil Current in the study region. Because of its pathway (Fig. 3), this contribution will depend on the latitude. An indication of this can be seen in Figure 4, where the agreements are best near the southern latitudes where the confluence with the Malvinas Current results in the separation of the Brazil Current from the shelf break. Based on the grid resolution of 0.5^o in Argo & SSH and the slope of the topography, 600 m is used in the following to split the Brazil Current transport into the shallow and open ocean contributions.

For the XBT transects, the analysis was done for two regions separated by the latitude of 27^{o}S. This latitude can be seen as representative for the transition from lower to higher transports. In addition, this latitude is the one where the integration depth transitions from 400 m to 800 m as explained in section 3. In the southern region, the the mean contribution of the shallow regions to the Brazil Current transport is 1.7±2.2 Sv (based on 20 transects). In 12% of the cases the transports are identical and an additional 44% of the cases have differences that do not exceed 10% of the transport in the Brazil Current. In the northern region, the mean contribution of the shallow regions to the Brazil Current transport is similar with 1.6±1.7 Sv (based on 8 transects). No further analysis is possible in this latitude range because of the small number of transects.

For HYCOM, the focus for quantifying the impact of the transport in shallow regions is on the three latitudes for which the time series are analyzed in detail. At 38^{o}S, the impact of the shallow areas on the transport is negligible (a mean difference that is insignificant; identical transports in 86% of the cases), because the Brazil Current is separated from the shelf break most of the time. At 24^{o}S, the impact of the shallow areas is slightly larger (mean difference of 0.7±1.3 Sv; identical transports in 67% of the cases). The largest impact exists at 35^{o}S, where the mean difference is 2.0±1.3 Sv (identical transports in only 14% of the cases). Overall, there is no statistical significant time dependence of the differences. All of these transport reductions are smaller than the differences between the transports from HYCOM and Argo & SSH (Table 1 and Fig. 5).